




Article

Half-Duplex Energy Harvesting Relay Network over Different Fading Environment: System Performance with Effect of Hardware Impairment

Duy-Hung Ha ^{1,2}, Si Thien Chau Dong ^{2,*}, Tan N. Nguyen ^{1,2}, Tran Thanh Trang ³ and Miroslav Voznak ¹

¹ Faculty of Electrical Engineering and Computer Science, VSB-Technical University of Ostrava 17, Listopadu 15/2172, 708 33 Ostrava-Poruba, Czech Republic; duy.hung.ha.st@vsb.cz (D.-H.H.); tan.nhat.nguyen.st@vsb.cz (T.N.N.); miroslav.voznak@vsb.cz (M.V.)

² Faculty of Electrical and Electronics Engineering, Ton Duc Thang University, Ho Chi Minh City 70000, Vietnam

³ Faculty of Engineering and Technology, Van Hien University, 665-667-669 Dien Bien Phu, Ho Chi Minh City 70000, Vietnam; trangtt@vhu.edu.vn

* Correspondence: dongsithienchau@tdtu.edu.vn

Received: 7 May 2019; Accepted: 24 May 2019; Published: 3 June 2019



Abstract: In this paper, we introduce a half-duplex (HD) energy harvesting (EH) relay network over the different fading environment with the effect of hardware impairment (HI). The model system was investigated with the amplify-and-forward (AF) and the power splitting (PS) protocols. The system performance analysis in term of the outage probability (OP), achievable throughput (AT), and bit error rate (BER) were demonstrated with the closed-form expressions. In addition, the power splitting (PS) factor was investigated. We verified the analytical analysis by Monte Carlo simulation with all primary parameters. From the results, we can state that the analytical and simulation results match well with each other.

Keywords: amplify-and-forward (AF); relay network; achievable throughput (AT); outage probability (OP); BER; energy harvesting (EH)

1. Introduction

Nowadays, wireless powered communication networks (WPCNs) have shown significant advantages in industry and living. The major benefits of WPCNs mainly come from battery charging operations through the air without physical cable connections and recharging, and thus, replacing the battery. As such, the maintenance, servicing, and charging of many battery-powered devices deployed in networks are crucially simplified, especially for future applications and technology [1–5]. Nowadays, there are three primary wireless energy harvesting (EH) and transfer techniques in the two main types of wireless charging—radiative (or RF based) and non-radiative (or coupling based) are employed in practice in WPCNs—which are feasible using the following techniques. In the first method, inductive coupling based on magnetic field induction can be used for transferring electrical energy over distances ranging from a few millimeters to a few centimeters. The efficiency of this method, from around 6% to 90%, is suitable for cell phone charging, contactless smart cards, and passive RFID cards [3,4]. Magnetic Resonant coupling is the second method, which is based on one vane scent wave coupling by making two separate coils resonate at the same frequency. Its efficiency ranges from 30% to around 90% and is suitable for plug-in hybrid electric vehicles and cell phone charging [3,4]. The last method is RF energy transfer, which is suitable for wireless body and wireless sensor networks. From this point of view, RF energy transfer WPCNs are suitable for long-distance transfers [1–5]. Some papers have

presented the process of EH through the RF signals in cooperative wireless networks using a MIMO relay system, and have investigated multi-user and multi-hop systems for simultaneous information and power transfer with a dual-hop channel [6–18]. In these previous papers, the authors have focused on WPCNs using only the Rayleigh or the Rician fading channel. However, to date not many papers concentrate on using both different fading channels. Hardware impairment (HI) suffers from phase noise, I/Q imbalance, and high-power amplifier nonlinearities [19–22]. HI is rarely studied in the literature on relay WPCNs.

In a wireless network, the source and destination may not communicate to each other directly, because the distance between the source and destination is greater than the transmission range of them both, hence the need for an intermediate node(s) to relay. Relaying is an effective way to combat the performance degradation caused by fading, shadowing, and path loss. In relay networks, the relay nodes help to boost the information exchange between source nodes and destination nodes, by forwarding (with or without decoding) the information-bearing radio frequency signals from sources to destinations [1–5]. In this paper, we introduce a half-duplex (HD) energy harvesting (EH) relay network over the different fading environment with the effect of hardware impairment (HI). The model system was investigated with the amplify-and-forward (AF) and the power-splitting (PS) protocols. The system performance analysis, in term of the outage probability (OP), achievable throughput (AT), and the bit error rate (BER), was analyzed and demonstrated with the closed-form expressions. Additionally, the power splitting (PS) factor was investigated. We verified the analytical analysis using a Monte Carlo simulation with all primary parameters. The research results showed that the analytical and simulation results matched well with each other. The main contributions are summarized as follow:

- (1) An HD EH relay network over the different fading environment (Rayleigh and Rician Fading Channel) with the HI effect of HI is introduced and investigated.
- (2) The closed form of OP, AT, and BER of the proposed system was analyzed and derived in connection with the main primary system parameters.
- (3) The correctness of the analytical expression was demonstrated by Monte Carlo simulation.

The remainder of this paper is introduced as follows. Section 2 introduces the system model with EH and information transmission (IT) phases. OP, AT, and BER are derived in Section 3. Section 4 shows and discusses the numerical results. Finally, Section 5 provides some conclusions.

2. System Model Network

An HD EH relay network over the different fading environment (Rayleigh and Rician Fading Channel), with the effect of HI, is illustrated in Figure 1. This system model is working in AF mode and PS protocol, in which the source (S) and destination (D) can exchange their signal via the helping Relay (R), as shown in Figure 1. The PS protocol of the system model is plotted in Figure 2. Here, T denotes the block time for EH and IT processes in the PS protocol. In the first half interval time $T/2$, the S simultaneously transfers information and energy to the R with the PS factor $\rho \in (0, 1)$, ρP is used for energy harvesting at the R and $(1 - \rho) P$ is used for transmitting information to the R node. So, the remaining $T/2$ interval time is used for transferring information from the R to the D [17–20].

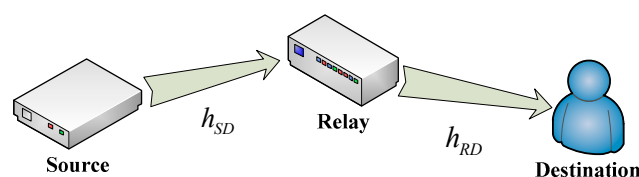


Figure 1. System model.

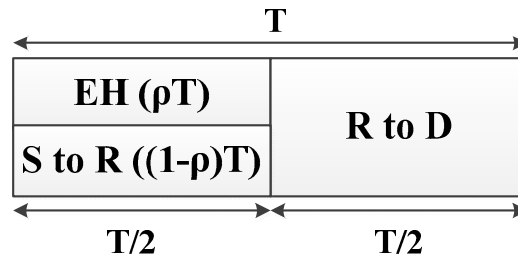


Figure 2. Power splitting (PS) protocol.

2.1. Energy Harvesting (EH)

The signal is transferred from the S to the R in the first-half $T/2$ and can be formulated as

$$y_r = h(x_s + \mu_s) + n_r \quad (1)$$

The received RF signal at the input of the energy harvesting unit can be calculated as

$$y_{h,r} = \sqrt{\rho} \times y_r = \sqrt{\rho} h x_s + \sqrt{\rho} h \mu_s + \sqrt{\rho} n_r \quad (2)$$

In this equation, x_s is the energy-transmitted signal with $E\{|x_s|^2\} = P_s$, n_r is the zero-mean additive white Gaussian noise (AWGN) with variance N_0 , and μ_s denotes the distortion error caused by hardware impairment at the source node, which is modeled as a zero-mean Gaussian random variable with variance $P_s \sigma_1^2$ with $E\{|\mu_s|^2\} = P_s \sigma_1^2$. Here $E\{\cdot\}$ denotes the expectation operation.

From Equation (2), the harvested energy at R in the first interval $T/2$ can be formulated as the following

$$E_h = \eta \rho P_s |h|^2 (T/2) \quad (3)$$

Therefore, the transmitted power at R can be calculated as

$$P_r = \frac{E_h}{T/2} = \frac{\eta \rho P_s |h|^2 (T/2)}{T/2} = \eta \rho P_s |h|^2 \quad (4)$$

where η is denoted the energy conversion efficiency of the proposed system.

2.2. Information Transmission (IT)

In this model, the IT phase is divided into two equal-length subintervals with the length $T/2$. In the first interval, we can calculate the received signal as

$$y_r = \sqrt{1-\rho} h (x_s + \mu_s) + n_r = \sqrt{1-\rho} h x_s + \sqrt{1-\rho} h \mu_s + n_r \quad (5)$$

where x_r is the transmitted signal, which satisfies $E\{|x_r|^2\} = P_r$, μ_r denotes the distortion error caused by hardware impairment at R, which is modeled as a zero-mean Gaussian random variable with variance $P_r \sigma_2^2$ and $E\{|\mu_r|^2\} = P_r \sigma_2^2$, and n_r is the AWGN noise at R node.

Here, we use the amplify-and-forward (AF) protocol for our model. Then, the received signal at R is amplified by a factor β , which is given by Equation (6)

$$\beta = \frac{x_r}{y_r} = \sqrt{\frac{P_r}{(1-\rho)|h|^2 P_s + (1-\rho)|h|^2 P_s \sigma^2 + N_0}} \quad (6)$$

In the remaining $T/2$ interval time, R transfers the information to D. Hence, the received signal at D node is formulated by

$$\begin{aligned}
y_d &= g(x_r + \mu_r) + n_D = gx_r + g\mu_r + n_d \\
&= g\beta y_r + g\mu_r + n_d \\
&= g\beta(\underbrace{\sqrt{1-\rho}hx_s}_{\text{signal}} + \underbrace{\sqrt{1-\rho}h\mu_s + n_r}_{\text{noise}}) + g\mu_r + n_D \\
&= g\beta\sqrt{1-\rho}hx_s + \sqrt{1-\rho}h\mu_s g\beta + g\beta n_r + g\mu_r + n_D
\end{aligned} \tag{7}$$

Here n_d is the noise at the destination, which is assumed to have the same power as n_r . The end-to-end signal-to-noise ratio (SNR) at D node can be given by

$$\gamma_{e2e} = \frac{E\{(signal)^2\}}{E\{(noise)^2\}} = \frac{(1-\rho)|g|^2\beta^2|h|^2P_s}{|g|^2\beta^2|h|^2P_s\sigma_1^2 + |g|^2\beta^2N_o + |g|^2P_r\sigma_2^2 + N_o} \tag{8}$$

We denote $\varphi_1 = |h|^2$, $\varphi_2 = |g|^2$ and replacing this in Equation (8), we have

$$\gamma_{e2e} = \frac{(1-\rho)\varphi_1\varphi_2\beta^2P_s}{\varphi_1\varphi_2\beta^2P_s\sigma_1^2 + \varphi_2\beta^2N_o + \varphi_2P_r\sigma_2^2 + N_o} \tag{9}$$

$$\begin{aligned}
\gamma_{e2e} &= \frac{(1-\rho)\varphi_1\varphi_2P_s}{\varphi_1\varphi_2P_s\sigma_1^2 + \varphi_2N_o + \frac{\varphi_2P_r\sigma_2^2}{\beta^2} + \frac{N_o}{\beta^2}} \\
&= ((1-\rho)\varphi_1\varphi_2P_s) / (\varphi_1\varphi_2P_s\sigma_1^2 + \varphi_2N_o + (1-\rho)\varphi_1\varphi_2P_s\sigma_2^2 + \\
&\quad (1-\rho)\varphi_1\varphi_2P_s\sigma_1^2\sigma_2^2 + \varphi_2N_o\sigma_2^2 + \frac{N_o(1-\rho)}{\eta\rho} + \frac{N_o(1-\rho)\sigma_1^2}{\eta\rho} + \frac{N_o^2}{P_r})
\end{aligned} \tag{10}$$

Because $N_o \ll P_r$, then we can reformulate Equation (10) as the following equation

$$\begin{aligned}
\gamma_{e2e} &= \{(1-\rho)\varphi_1\varphi_2P_s\} / \{\varphi_1\varphi_2P_s\sigma_1^2 \\
&\quad + \varphi_2N_o + (1-\rho)\varphi_1\varphi_2P_s\sigma_2^2 + (1-\rho)\varphi_1\varphi_2P_s\sigma_1^2\sigma_2^2 \\
&\quad + \varphi_2N_o\sigma_2^2 + \frac{N_o(1-\rho)}{\eta\rho} + \frac{N_o(1-\rho)\sigma_1^2}{\eta\rho}\}
\end{aligned} \tag{11}$$

$$\begin{aligned}
\gamma_{e2e} &= \{(1-\rho)\varphi_1\varphi_2\gamma_0\} / \{\varphi_1\varphi_2\gamma_0\sigma_1^2 \\
&\quad + \varphi_2 + (1-\rho)\varphi_1\varphi_2\gamma_0\sigma_2^2 \\
&\quad + (1-\rho)\varphi_1\varphi_2\gamma_0\sigma_1^2\sigma_2^2 + \varphi_2\sigma_2^2 + \kappa + \kappa\sigma_1^2\}
\end{aligned} \tag{12}$$

where we denote $\kappa = \frac{1-\rho}{\eta\rho}$, $\gamma_0 = \frac{P_s}{N_o}$.

In the next section, we analyze the achievable throughput (AT), outage probability (OP) and BER in AF mode with the PS protocol [6–8].

3. System Model Performance

In this section, we investigate the system performance of the relay network with the PS protocol [10–13,23–27]. In this analysis, we consider two Scenarios: (1) S-R link is the Rayleigh Fading Channel and R-D link is Rician Fading Channel, and (2) S-R link is the Rician Fading Channel and R-D link is the Rayleigh Fading Channel.

3.1. Scenario 1: S-R link Is Rayleigh Fading Channel, R-D link Is Rician Fading Channel

As in previous studies [6–9], the probability density function (PDF) of a random variable (RV) φ_1 can be written as the following equation

$$f_{\varphi_1}(x) = \lambda_h e^{-\lambda_h x} \tag{13}$$

Here λ_h is the mean value of RV φ_1 .

The cumulative density function (CDF) of RV φ_1 can be written as

$$F_{\varphi_1}(x) = 1 - e^{-\lambda_h x} \quad (14)$$

Similarly, the PDF of RV φ_2 can be obtained as in [26], giving

$$f_{\varphi_2}(x) = \frac{(K+1)e^{-K}}{\lambda_g} e^{-\frac{(K+1)x}{\lambda_g}} I_0 \left(2 \sqrt{\frac{K(K+1)x}{\lambda_g}} \right) \quad (15)$$

where λ_g is the mean value of RV φ_2 , K denotes the Rician K -factor, and $I_0(\bullet)$ is the zero-th order modified Bessel function of the first kind [26].

Then the Equation (14) can be reformulated as the following

$$f_{\varphi_2}(x) = a \sum_{l=0}^{\infty} \frac{(bK)^l}{(l!)^2} x^l e^{-bx} \quad (16)$$

where we denote $a = \frac{(K+1)e^{-K}}{\lambda_g}$, $b = \frac{K+1}{\lambda_g}$ and $I_0(x) = \sum_{l=0}^{\infty} \frac{x^{2l}}{2^{2l}(l!)^2}$ [24].

The cumulative density function (CDF) of RV φ_2 can be computed like in [27]

$$F_{\varphi_2}(\varsigma) = \int_0^{\varsigma} f_{\varphi_2}(x) dx = 1 - \frac{a}{b} \sum_{l=0}^{\infty} \sum_{m=0}^l \frac{K^l b^m}{l! m!} \varsigma^m e^{-b\varsigma} \quad (17)$$

After that, the OP of the proposed system can be computed as

$$P_{out} = F_{\gamma_{e2e}}(\gamma) = \Pr(\gamma_{e2e} < \gamma) \quad (18)$$

If we denote $\gamma = 2^R - 1$ to be the lower threshold for SNR at both R and D, and R is fixed transmission rate at S, then Equation (18) can be reformulated as the following

$$P_{out} = \Pr \left\{ \begin{array}{l} \varphi_1 \varphi_2 \gamma_0 [1 - \rho - \gamma \sigma_1^2 - \gamma(1 - \rho) \sigma_2^2 \\ - \gamma(1 - \rho) \sigma_1^2 \sigma_2^2] < \varphi_2 (\gamma + \gamma \sigma_2^2) + \gamma \kappa + \gamma \kappa \sigma_1^2 \end{array} \right\} \quad (19)$$

Here we denote $c_1 = \gamma + \gamma \sigma_2^2$, $c_2 = \gamma \kappa + \gamma \kappa \sigma_1^2$, and $c_3 = \gamma_0 [1 - \rho - \gamma \sigma_1^2 - \gamma(1 - \rho) \sigma_2^2 - \gamma(1 - \rho) \sigma_1^2 \sigma_2^2]$. We assume that c_3 is positive, because if c_3 is negative, the OP of the system is always equal to 1.

a. Outage Probability (OP)

$$P_{out} = \Pr \left\{ \varphi_1 < \frac{c_1 \varphi_2 + c_2}{c_3 \varphi_2} \right\} = \int_0^{\infty} F_{\varphi_1} \left(\frac{c_1 \varphi_2 + c_2}{c_3 \varphi_2} \right) f_{\varphi_2}(\varphi_2) d\varphi_2 \quad (20)$$

Combining Equation (20) with Equations (14) and (17) we have

$$P_{out} = 1 - \int_0^{\infty} e^{-\lambda_h \frac{c_1 \varphi_2 + c_2}{c_3 \varphi_2}} \times a \sum_{l=0}^{\infty} \frac{(bK)^l}{(l!)^2} \varphi_2^l e^{-b\varphi_2} d\varphi_2 = 1 - ae^{-\frac{\lambda_h c_1}{c_3}} \sum_{l=0}^{\infty} \frac{(bK)^l}{(l!)^2} \int_0^{\infty} \varphi_2^l e^{-b\varphi_2} e^{-\frac{\lambda_h c_2}{c_3 \varphi_2}} d\varphi_2 \quad (21)$$

Using Table of Integral Equation [3.471,9] in [24], Equation (21) can be given as

$$P_{out} = 1 - 2ae^{-\frac{\lambda_h c_1}{c_3}} \sum_{l=0}^{\infty} \frac{(bK)^l}{(l!)^2} \left(\frac{\lambda_h c_2}{c_3 b} \right)^{\frac{l+1}{2}} \times K_{l+1} \left(2 \sqrt{\frac{\lambda_h c_2 b}{c_3}} \right) \quad (22)$$

where $K_v(\bullet)$ is the modified Bessel function of the second kind and v^{th} order.

b. Achievable Throughput (AT)

Here, the average throughput of the relay network system can be computed regarding the OP as in Equation (23)

$$\tau = (1 - P_{out}) \frac{R}{2} = 2ae^{-\frac{\lambda_h c_1}{c_3}} \sum_{l=0}^{\infty} \frac{(bK)^l}{(l!)^2} \left(\frac{\lambda_h c_2}{c_3 b} \right)^{\frac{l+1}{2}} \times K_{l+1} \left(2 \sqrt{\frac{\lambda_h c_2 b}{c_3}} \right) \times \frac{R}{2} \quad (23)$$

c. The Bit Error Rate (BER)

The BER of the proposed system can be formulated from the expression of the OP as the following equation

$$BER = E[\omega Q(\sqrt{2\theta\gamma})] \quad (24)$$

where $Q(t) = \frac{1}{\sqrt{2\pi}} \int_t^{\infty} e^{-x^2/2} dx$ is the Gaussian Q-function, ω and θ are constants which are specific for modulation type. Here, we use $(\omega, \theta) = (1, 2)$ for BPSK and $(\omega, \theta) = (1, 1)$ for QPSK. Hence, we begin rewriting the BER expression in Equation (24) directly regarding OP at S by using integration as in the equation below

$$BER = \frac{\omega \sqrt{\theta}}{2 \sqrt{\pi}} \int_0^{\infty} \frac{e^{-\theta x}}{\sqrt{x}} F_{\gamma_{e2e}}(x) dx \quad (25)$$

3.2. Scenario 2: S-R Link Is the Rician Fading Channel, R-D Link Is the Rayleigh Fading Channel

Similar to scenario 1, the CDF of RV φ_1 and PDF of RV φ_2 can be formulated as

$$F_{\varphi_1}(\varsigma) = \int_0^{\varsigma} f_{\varphi_1}(x) dx = 1 - \frac{a}{b} \sum_{l=0}^{\infty} \sum_{m=0}^l \frac{K^l b^m}{l! m!} \varsigma^m e^{-b\varsigma} \quad (26)$$

where $a = \frac{(K+1)e^{-K}}{\lambda_h}$, $b = \frac{K+1}{\lambda_h}$

$$f_{\varphi_2}(x) = \lambda_g e^{-\lambda_g x} \quad (27)$$

a. Outage Probability (OP)

$$P_{out} = \Pr \left\{ \varphi_1 < \frac{c_1 \varphi_2 + c_2}{c_3 \varphi_2} \right\} = \int_0^{\infty} F_{\varphi_1} \left(\frac{c_1 \varphi_2 + c_2}{c_3 \varphi_2} \right) f_{\varphi_2}(\varphi_2) d\varphi_2 \quad (28)$$

$$P_{out} = 1 - \int_0^{\infty} \frac{a}{b} \sum_{l=0}^{\infty} \sum_{m=0}^l \frac{K^l b^m}{l! m!} \left(\frac{c_1 \varphi_2 + c_2}{c_3 \varphi_2} \right)^m e^{-\frac{b(c_1 \varphi_2 + c_2)}{c_3 \varphi_2}} \lambda_g e^{-\lambda_g \varphi_2} d\varphi_2 \quad (29)$$

We apply the equation $(x + y)^m = \sum_{n=0}^m \binom{m}{n} x^{m-n} y^n$, and change the variable by setting, and Equation (27) can be reformulated as the following

$$P_{out} = 1 - \lambda_g e^{-\frac{bc_1}{c_3}} \int_0^{\infty} \frac{a}{b} \sum_{l=0}^{\infty} \sum_{m=0}^l \sum_{n=0}^m \binom{m}{n} \frac{K^l b^m c_1^{m-n} c_2^n}{l! m! c_3^m} t^{n-2} e^{-\frac{bc_2 t}{c_3}} e^{-\frac{\lambda_g}{t}} dt \quad (30)$$

$$P_{out} = 1 - \lambda_g e^{-\frac{bc_1}{c_3}} \frac{a}{b} \sum_{l=0}^{\infty} \sum_{m=0}^l \sum_{n=0}^m \frac{K^l b^m c_1^{m-n} c_2^n}{l! n! (m-n)! c_3^m} \int_0^{\infty} t^{n-2} e^{-\frac{bc_2 t}{c_3}} e^{-\frac{\lambda_g}{t}} dt \quad (31)$$

Using the Table of Integral Equation [3.471,9] in [24], the above equation can be given as

$$P_{out} = 1 - 2\lambda_g e^{-\frac{bc_1}{c_3}} \frac{a}{b} \sum_{l=0}^{\infty} \sum_{m=0}^l \sum_{n=0}^m \frac{K^l b^m c_1^{m-n} c_2^n}{l! n! (m-n)! c_3^m} \left(\frac{\lambda_g c_3}{bc_2} \right)^{\frac{n-1}{2}} K_{n-1} \left(2 \sqrt{\frac{bc_2 \lambda_g}{c_3}} \right) \quad (32)$$

$$P_{out} = 1 - 2ae^{-\frac{bc_1}{c_3}} \sum_{l=0}^{\infty} \sum_{m=0}^l \sum_{n=0}^m \frac{K^l b^{\frac{2m-n-3}{2}} \lambda_g^{\frac{n+1}{2}} c_1^{m-n} c_2^{\frac{n+1}{2}} c_3^{\frac{n-1-2m}{2}}}{l! n! (m-n)!} \times K_{n-1} \left(2 \sqrt{\frac{bc_2 \lambda_g}{c_3}} \right) \quad (33)$$

where $K_v(\bullet)$ is the modified Bessel function of the second kind and v^{th} order.

b. Achievable Throughput (AT):

$$\tau = (1 - P_{out}) \frac{R}{2} = 2ae^{-\frac{bc_1}{c_3}} \sum_{l=0}^{\infty} \sum_{m=0}^l \sum_{n=0}^m \frac{K^l b^{\frac{2m-n-3}{2}} \lambda_g^{\frac{n+1}{2}} c_1^{m-n} c_2^{\frac{n+1}{2}} c_3^{\frac{n-1-2m}{2}}}{l! n! (m-n)!} \times K_{n-1} \left(2 \sqrt{\frac{bc_2 \lambda_g}{c_3}} \right) \times \frac{R}{2} \quad (34)$$

c. The Bit Error Rate (BER)

Similar to scenario 1, BER can be calculated with the equation below

$$BER = \frac{\omega \sqrt{\theta}}{2 \sqrt{\pi}} \int_0^{\infty} \frac{e^{-\theta x}}{\sqrt{x}} F_{\gamma_{e2e}}(x) dx \quad (35)$$

3.3. Optimal Power-Splitting (PS) Factor

In this section, we can calculate the optimal value ρ^* by solving the equation $\frac{d\tau(\rho)}{d\rho} = 0$, using the AT expression in Equations (23) and (34). Here, we use the Golden section search algorithm as in [25,28–30], which is popularly used in many global optimization problems in communications.

4. Results and Discussion

In this section, we investigate the system performance in terms of OP, AT, BER, and the PS factor in connection with the main system parameters: η , ρ , P_s/N_0 and σ_1 , σ_2 . The primary system simulation parameters are listed in Table 1.

Table 1. The main simulation parameters.

Symbol	Name	Values
η	Energy harvesting efficiency	0.7
λ_h	Mean of $ h ^2$	0.5
λ_g	Mean of $ g ^2$	0.5
K	Rician K-factor	3
γ_{th}	SNR threshold	7
P_s/N_0	Source power-to-noise ratio	0–30 dB
σ_1	Distortion error	0.01
σ_2	Distortion error	0.05
R	Source rate	3 bit/s/Hz

Figures 3 and 4 plot the OP and AT versus the energy conversion efficiency η . The effect of η was investigated in both scenarios, and we vary η continuously from 0 to 1. From the figures, we can see that the OP decreased and the AT increased crucially with η varying from 0 to 1; and the OP and AT in the second case is better than in the first case. Furthermore, the results show the correctness of the simulation and analytical expressions. Moreover, Figures 5 and 6 plot the impact of the ratio P_s/N_0 on the OP and AT, while the ratio P_s/N_0 increases from 0 to 30 dB. From the research results, we can state that the OP decreased and AT increased with the rising of the ratio P_s/N_0 , and the analytical results match very well with the analytical values.

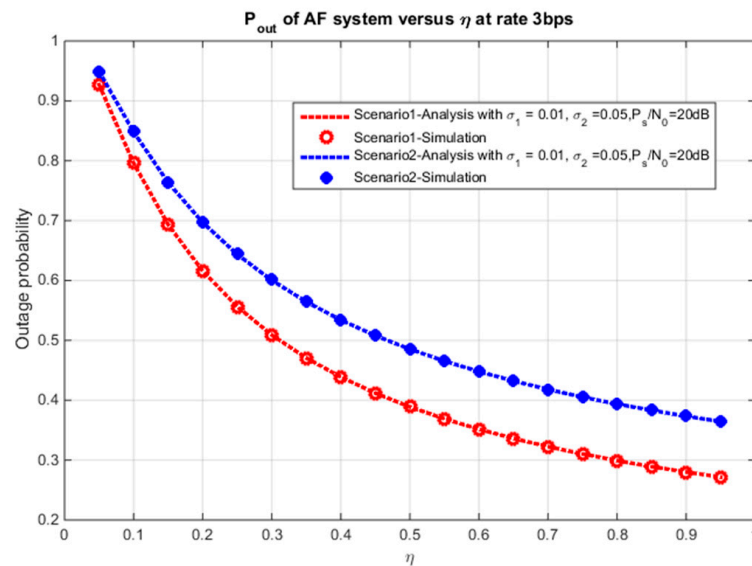


Figure 3. Outage probability versus η .

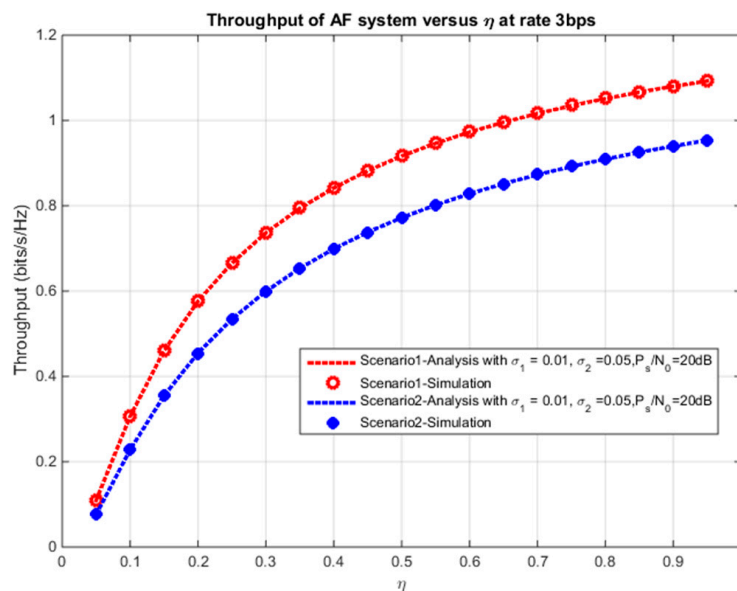


Figure 4. The throughput versus η .

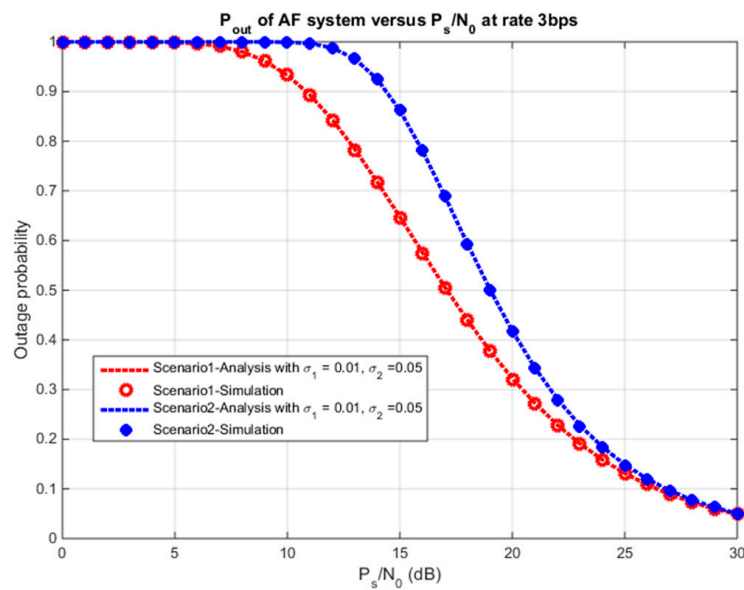


Figure 5. The outage probability versus ratio of P_s/N_0 .

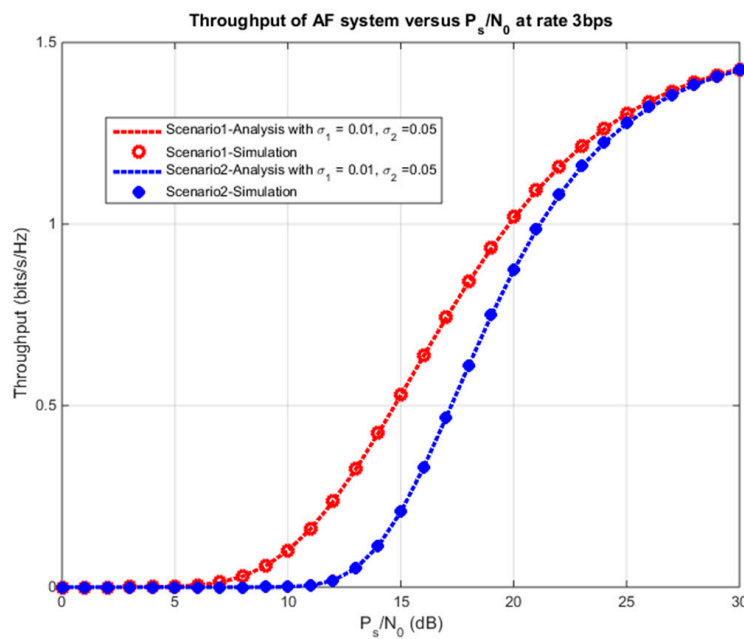


Figure 6. The throughput versus ratio P_s/N_0 .

In addition, the OP and AT versus the PS factor ρ are shown in Figures 7 and 8. It can be observed that the AT increased and OP fell at the D with factor ρ from 0 to 0.6. After that, the OP and AT had the opposite effect when ratio ρ from 0.6 to 1.0. We can find the optimal value of factor ρ from 0.6 to 0.7 in this situation. It can be observed that when ρ is too small, R cannot harvest enough energy from S to operate reliably, but when ρ is too large then the reliability of the communications link from S to R is impaired. Furthermore, the OP and AT of the model system versus $\sigma_1 = \sigma_2$ varied from 0 to 0.2 and are plotted in Figures 9 and 10. In the same way, OP increased and AT decreased with the increasing of $\sigma_1 = \sigma_2$. In all the above figures, the simulation and analytical results agree well with each other.

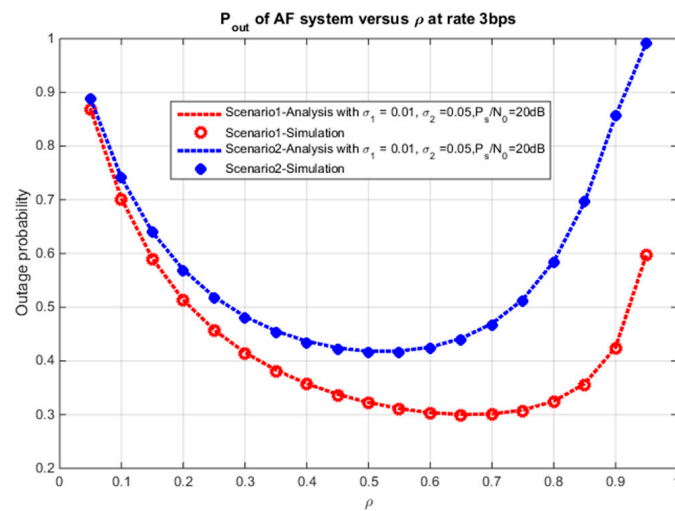


Figure 7. The outage probability versus ρ for the PS protocol.

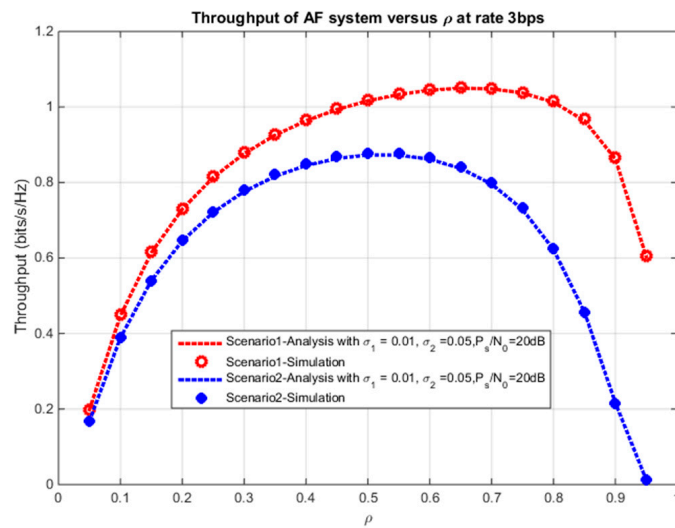


Figure 8. The throughput versus ρ for the PS protocol.

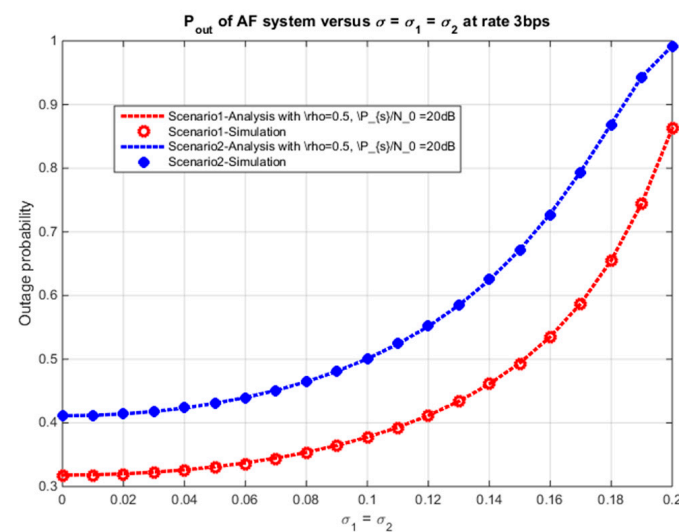


Figure 9. The outage probability versus $\sigma_1 = \sigma_2$.

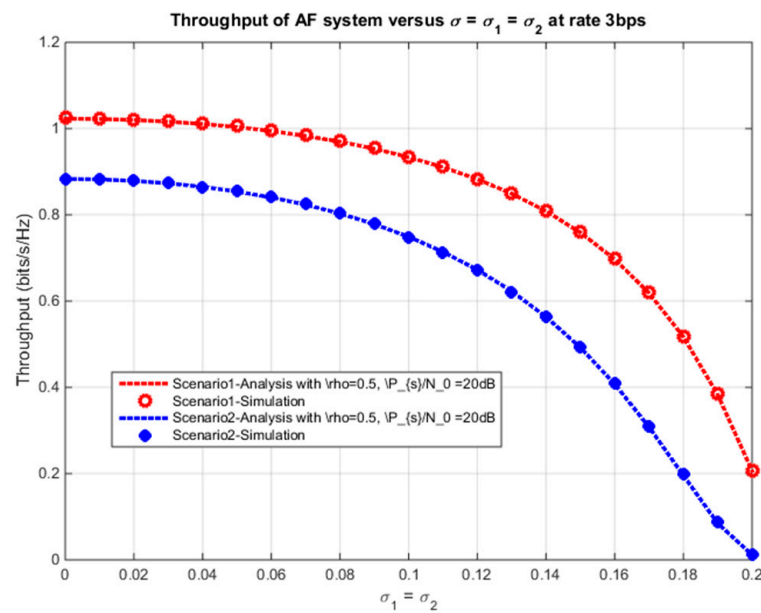


Figure 10. The throughput versus $\sigma_1 = \sigma_2$.

Figures 11 and 12 show the optimal PS factor versus the ratio P_s/N_0 in both scenarios. As shown in the figures, the optimal power splitting factor increased while the ratio P_s/N_0 varied from 0 to 30 dB. Moreover, Figure 13 plots the dependent of BER on the ratio P_s/N_0 . The results show that BER decreased significantly with P_s/N_0 from 0 to 20 dB. After that, BER slightly decreased.

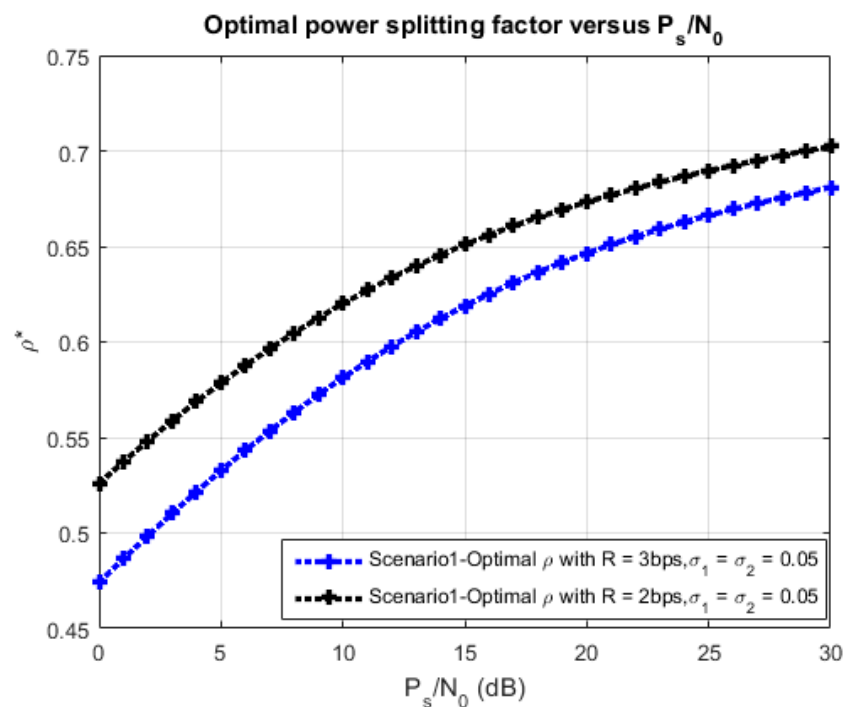


Figure 11. The optimal PS factor versus P_s/N_0 for the first case.

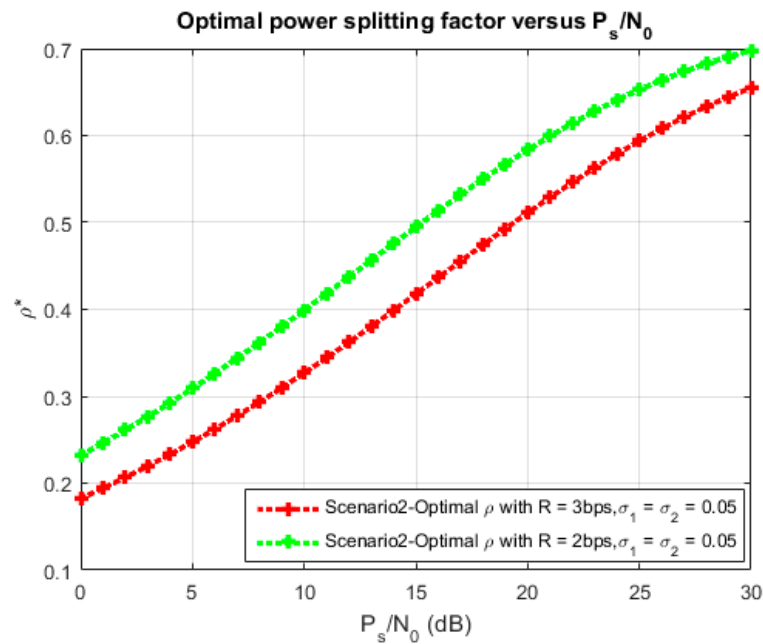


Figure 12. The optimal PS factor versus P_s/N_0 for the second case.

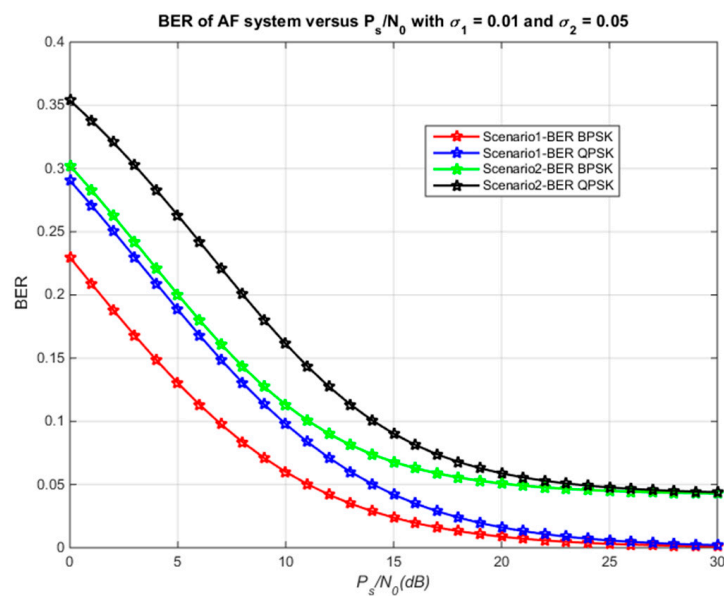


Figure 13. BER versus the ratio P_s/N_0 .

5. Conclusions

In this paper, we propose and investigate the system performance of an AF wireless network over the different fading channel. The system model is considered under the effect of hardware impairment with the PS protocols. Firstly, the closed-form expressions of OP, AT, and BER of the proposed system is analyzed and derived. After that, we used the Monte Carlo simulation to verify the correctness of the analytical expressions in connection with the primary system parameters. Finally, the numerical results show that the analytical mathematical expression and the simulation results using the Monte Carlo method are in agreement with each other. In addition, the optimal PS factor was investigated in both cases.

Author Contributions: Methodology, D.H.H.; software, N.T.N, D.H.H.; validation, T.T.T, D.H.H; writing—original draft preparation, S.T.C.D.; writing—review and editing, S.T.C.D.; supervision, M.V.

Funding: This research was funded by the Czech Ministry of Education, Youth and Sports within the grants No. SP2018/59 and SP2019/41 conducted at the VSB—Technical University of Ostrava.

Conflicts of Interest: The authors declare no conflict of interest.

References

- Chen, X.; Ng, D.W.K.; Chen, H.-H. Secrecy Wireless Information and Power Transfer: Challenges and Opportunities. *IEEE Wirel. Commun.* **2016**, *23*, 54–61. [\[CrossRef\]](#)
- Bi, S.; Ho, C.K.; Zhang, R. Wireless powered communication: Opportunities and challenges. *IEEE Commun. Mag.* **2015**, *53*, 117–125. [\[CrossRef\]](#)
- Niyato, D.; Kim, D.I.; Maso, M.; Han, Z. Wireless Powered Communication Networks: Research Directions and Technological Approaches. *IEEE Wirel. Commun.* **2017**, *24*, 88–97. [\[CrossRef\]](#)
- Atallah, R.; Khabbaz, M.; Assi, C. Energy harvesting in vehicular networks: A contemporary survey. *IEEE Wirel. Commun.* **2016**, *23*, 70–77. [\[CrossRef\]](#)
- Liu, L.; Zhang, R.; Chua, K. Wireless Information and Power Transfer: A Dynamic Power Splitting Approach. *IEEE Trans. Commun.* **2013**, *61*, 3990–4001. [\[CrossRef\]](#)
- Sharma, V.; Karmakar, P. A Novel Method of Opportunistic Wireless Energy Harvesting in Cognitive Radio Networks. In Proceedings of the 2015 7th International Conference on Computational Intelligence, Communication Systems and Networks, Riga, Latvia, 3–5 June 2015. [\[CrossRef\]](#)
- Fouladgar, A.M.; Simeone, O. On the Transfer of Information and Energy in Multi-User Systems. *IEEE Commun. Lett.* **2012**, *16*, 1733–1736. [\[CrossRef\]](#)
- Zhang, R.; Ho, C.K. MIMO Broadcasting for Simultaneous Wireless Information and Power Transfer. *IEEE Trans. Wirel. Commun.* **2013**, *12*, 1989–2001. [\[CrossRef\]](#)
- Park, J.; Clerckx, B. Joint Wireless Information and Energy Transfer in a Two-User MIMO Interference Channel. *IEEE Trans. Wirel. Commun.* **2013**, *12*, 4210–4221. [\[CrossRef\]](#)
- Do, D.-T.; Van Nguyen, M.-S.; Hoang, T.-A.; Voznak, M. NOMA-Assisted Multiple Access Scheme for IoT Deployment: Relay Selection Model and Secrecy Performance Improvement. *Sensors* **2019**, *19*, 736. [\[CrossRef\]](#) [\[PubMed\]](#)
- Nasir, A.A.; Zhou, X.; Durrani, S.; Kennedy, R.A. Relaying Protocols for Wireless Energy Harvesting and Information Processing. *IEEE Trans. Wirel. Commun.* **2013**, *12*, 3622–3636. [\[CrossRef\]](#)
- Do, D.-T.; Le, C.-B. Application of NOMA in Wireless System with Wireless Power Transfer Scheme: Outage and Ergodic Capacity Performance Analysis. *Sensors* **2018**, *18*, 3501. [\[CrossRef\]](#) [\[PubMed\]](#)
- Bhatnagar, M.R. On the Capacity of Decode-and-Forward Relaying over Rician Fading Channels. *IEEE Commun. Lett.* **2013**, *17*, 1100–1103. [\[CrossRef\]](#)
- Nguyen, X.-X.; Do, D.-T. Optimal power allocation and throughput performance of full-duplex DF relaying networks with wireless power transfer-aware channel. *EURASIP J. Wirel. Commun. Netw.* **2017**, *2017*, 152. [\[CrossRef\]](#)
- Nguyen, T.N.; Minh, T.H.Q.; Nguyen, T.-L.; Ha, D.-H.; Voznak, M. Performance Analysis of User Selection Protocol in Cooperative Networks with Power Splitting Protocol Based Energy Harvesting Over Nakagami-m/Rayleigh Channel. *Electronics* **2019**, *8*, 448. [\[CrossRef\]](#)
- Nguyen, T.N.; Minh, T.H.Q.; Nguyen, T.-L.; Ha, D.-H.; Voznak, M. Multi-Source Power Splitting Energy Harvesting Relaying Network In Half-Duplex System Over Block Rayleigh Fading Channel: System Performance Analysis. *Electronics* **2019**, *8*, 67. [\[CrossRef\]](#)
- Li, T.; Fan, P.; Letaief, K.B. Outage Probability of Energy Harvesting Relay-Aided Cooperative Networks Over Rayleigh Fading Channel. *IEEE Trans. Veh. Technol.* **2016**, *65*, 972–978. [\[CrossRef\]](#)
- Salhab, A.M.; Zummo, S.A. Cognitive Amplify-and-Forward Relay Networks with Switch-and-Examine Relaying in Rayleigh Fading Channels. *IEEE Commun. Lett.* **2014**, *18*, 825–828. [\[CrossRef\]](#)
- Nguyen, T.N.; Tin, P.T.; Ha, D.H.; Voznak, M.; Tran, P.T.; Tran, M.; Nguyen, T.-L. Hybrid TSR-PSR Alternate Energy Harvesting Relay Network over Rician Fading Channels: Outage Probability and SER Analysis. *Sensors* **2018**, *18*, 3839. [\[CrossRef\]](#)
- Matthaiou, M.; Papadogiannis, A.; Bjornson, E.; Debbah, M. Two-Way Relaying Under the Presence of Relay Transceiver Hardware Impairments. *IEEE Commun. Lett.* **2013**, *17*, 1136–1139. [\[CrossRef\]](#)

21. Younas, T.; Li, J.; Arshad, J. On Bandwidth Efficiency Analysis for LS-MIMO with Hardware Impairments. *IEEE Access* **2017**, *5*, 5994–6001. [[CrossRef](#)]
22. Miridakis, N.I.; Tsiftsis, T.A. On the Joint Impact of Hardware Impairments and Imperfect CSI on Successive Decoding. *IEEE Trans. Veh. Technol.* **2017**, *66*, 4810–4822. [[CrossRef](#)]
23. Duy, T.T.; Son, V.N.; Tung, V.T.; Alexandropoulos, G.C.; Duong, T.Q. Outage Performance of Cognitive Cooperative Networks with Relay Selection over Double-Rayleigh Fading Channels. *IET Commun.* **2016**, *10*, 57–64. [[CrossRef](#)]
24. *Table of Integrals, Series, and Products*; Academic Press: Cambridge, MA, USA, 2015. [[CrossRef](#)]
25. Chong, E.K.P.; Zak, S.H. *An Introduction to Optimization*; Wiley: Hoboken, NJ, USA, 2013.
26. Suraweera, H.; Karagiannidis, G.; Smith, P. Performance Analysis of the Dual-hop Asymmetric Fading Channel. *IEEE Trans. Wirel. Commun.* **2009**, *8*, 2783–2788. [[CrossRef](#)]
27. Nguyen, T.; Quang Minh, T.; Tran, P.; Vozňák, M. Energy Harvesting over Rician Fading Channel: A Performance Analysis for Half-Duplex Bidirectional Sensor Networks under Hardware Impairments. *Sensors* **2018**. [[CrossRef](#)] [[PubMed](#)]
28. Goldsmith, A. *Wireless Communications*; Cambridge University Press: Cambridge, UK, 2009.
29. Duong, T.Q.; Duy, T.T.; Matthaiou, M.; Tsiftsis, T.; Karagiannidis, G.K. Cognitive Cooperative Networks in Dual-hop Asymmetric Fading Channels. In Proceedings of the 2013 IEEE Global Communications Conference (GLOBECOM), Atlanta, GA, USA, 9–13 December 2013. [[CrossRef](#)]
30. Nguyen, T.N.; Minh, T.H.Q.; Tran, P.T.; Voznak, M.; Duy, T.T.; Nguyen, T.L.; Tin, P.T. Performance Enhancement for Energy Harvesting Based Two-Way Relay Protocols in Wireless Ad-hoc Networks with Partial and Full Relay Selection Methods. *Ad Hoc Netw.* **2019**. [[CrossRef](#)]



© 2019 by the authors. Licensee MDPI, Basel, Switzerland. This article is an open access article distributed under the terms and conditions of the Creative Commons Attribution (CC BY) license (<http://creativecommons.org/licenses/by/4.0/>).